Two-variable anharmonic model for spin-crossover solids: A like-spin domains interpretation

W. Nicolazzi, S. Pillet,* and C. Lecomte
Laboratoire de Cristallographie et Modélisation des Matériaux Minéraux et Biologiques, UMR CNRS 7036, Institut Jean Barriol, Nancy-Université, BP 239, F-54506 Vandoeuvre-lès-Nancy, France

(Received 9 June 2008; revised manuscript received 4 September 2008; published 4 November 2008)

Spin-crossover (SC) complexes are one of the most fascinating examples of molecular bistability, whose solid-state properties are tightly connected to cooperative interactions within the crystal lattice. A variety of macroscopic and microscopic models have been developed to explore the cooperative nature of the SC phenomenon. We present here a two-variable microscopic Ising-like model for SC solids, accounting for the elastic origin of the cooperativity using coupled spin and translational (lattice) degrees of freedom. Within our model, the interaction between a pair of neighboring molecules in the crystal is dependent not only on their spin states but also on their separation distance, modeled by spin-dependent Lennard-Jones (LJ) potentials. This scheme leads explicitly to local variations in the interactions, associated to the local strain induced by the molecules changing their spin state. In essence, the LJ potentials provide the anharmonicity of the crystal lattice. The equilibrium (quasistatic) properties of the proposed Hamiltonian are analyzed by Monte Carlo simulations on a regular deformable square lattice. We show that the spin dependence of the LJ potentials breaks the spin-state symmetry in the free energy. The interplay between spin and lattice degrees of freedom shows itself in the temperature evolution of the fraction of high-spin molecules and the mean lattice spacing, as a function of the intersite coupling. For strong coupling, like-spin domains nucleate and develop, evidenced by a double structure in the distribution of lattice spacings; structural relaxation occurs at the domain walls. In the weakly cooperative situation, the mean lattice constant scales directly with the fraction of high-spin species; structural relaxation spans the entire system.

DOI: 10.1103/PhysRevB.78.174401 PACS number(s): 05.50.+q, 64.60.De, 75.30.Wx, 75.60.−d

I. INTRODUCTION

The thermally induced spin-crossover (SC) phenomenon between the low-spin (LS) and the high-spin (HS) states of Fe(II) molecular complexes has been the subject of intense research activities.[1,2] The intrinsic bistability that these materials exhibit originates from intramolecular vibronic coupling. The higher electronic and vibrational degeneracy in the HS state leads to a LS to HS entropy increase, which drives the spin conversion. In addition to large variations in the magnetic and optical properties upon the spin-state change, drastic structural modifications occur, namely, a typical ≈0.2 Å Fe-N bond lengthening and a 2%–5% unit cell expansion.[3] Besides temperature or pressure changes, the spin conversion may alternatively be triggered by continuous light excitation, albeit at very low temperature [light-induced excited-spin-state trapping (LIESST) process],[4–6] and also at higher temperature within the thermal hysteresis loop by means of an intense pulsed laser.[7,8] Owing to their temperature- and light-induced switching potential, it is well established that these molecular systems may have prospective use as sensors or may be integrated in data storage devices.

In the solid state, strong electron-lattice coupling is at the origin of the rich variety of behaviors SC materials exhibit, such as gradual (spin crossover) or abrupt spin conversion (first-order character) with often hysteresis in the case of strongly cooperative materials. Although the concept is rather ill defined, cooperativity is often attributed to the large HS to LS molecular volume change coupled to elastic interactions within the solid. In the framework of the continuum elasticity theory, it has been pictured as the buildup of an internal pressure, proportional to the concentration of LS species.[9–11] The local distortion (strain) of the crystal lattice accompanying the spin transition has been traced back to point defects at the iron site of the spin-changing molecule. Cooperativity shows itself in the abruptness of the thermal transition and low-temperature sigmoidal HS to LS relaxation curves, attributed to a self-accelerated process.[12,13] Polymeric SC materials with one-dimensional (1D) chain or two-dimensional (2D) layer structural architectures are emblematic examples of highly cooperative systems, with sometimes extremely wide thermal hysteresis.[14] In that case, the bridging ligands play the role of efficient spin-state propagators and contribute to the anisotropic elasticity. On the other hand, for SC systems built from purely monomolecular entities, it is quite clear that the intermolecular contacts, through weak van der Waals, hydrogen bonds, or π-π stacking, transmit the interactions to long range and are thus responsible for the elastic properties of the solid.[15]

Intensive theoretical investigations have been devoted to the development of more or less sophisticated models of spin transition, treating cooperativity through various schemes. Among others, macroscopic models based on the thermodynamic theory of regular solutions were proposed. In the so-called Slichter and Drickamer (SD) model, cooperativity is described in mean field through phenomenological enthalpy terms related to the intermolecular interactions.[16] In the elastic model for SC systems introduced by Spiering and Willenbacher,[9–11] SC molecules are considered as entities whose volume and shape depend on their spin state, inserted in an isotropic elastic medium. When a molecule undergoes the spin transition, it creates a local strain which forces the nearest-neighbor molecules to undergo the spin transition as well (ferroelastic coupling). In its more elaborated form, the

Spiering scheme describes the crystal lattice within the Debye approximation and allows for anharmonicity through the Grüneisen approximation.[11,17] A variety of microscopic Ising-like models were also designed, introducing a Hamiltonian of interacting two-level units with different energies and degeneracies, as proposed by Wajnflasz and Pick[18,19] and Bousseksou *et al.*[20] These models can reproduce most of the equilibrium properties of SC materials as well as their dynamic behavior, including the sigmoidal relaxation, the two-step transitions, and the photoinduced effects.[21–27] The isomorphism between the macroscopic SD and microscopic Ising-like model in the mean field has been formulated.[24,28] A direct relation between the Ising coupling constant J and the phenomenological cooperative factor Γ in the SD scheme has been derived. The 1D version of the Ising-like model has been further solved analytically.[29] An alternative one-dimensional model of SC molecules coupled to a phonon field (atom-phonon coupling model) was established, the intermolecular interactions being introduced as harmonic springs.[30,31] This 1D model was recently solved analytically[32] and further extended to anharmonic contributions.[33] Various elastic models, for which the coupling constant depends on the intersite separation distance, have been proposed and investigated numerically through molecular dynamics (MD) methods[34,35] and Monte Carlo (MC) simulations.[36,37]

The mechanism by which the spin conversion proceeds in the solid state is a fundamental question. In the case of cooperative materials, characterized by an abrupt thermal transition and sigmoidal relaxation kinetics, it has been widely argued that molecule clustering may play a key role. The very first experiments which have indirectly observed so-called like-spin domains (LSDs) are powder and single-crystal diffraction measurements.[38–41] These techniques are by no way sensitive to the molecular spin component but on the contrary to lattice (structural) observables. In these experiments, LSD shows itself at the thermally and light-induced transitions by a clear separation of Bragg peaks corresponding to ordered HS and LS phases with different cell constants (phase separation). Within this framework, a domain consists of adjacent molecules, crystallographically ordered to sufficiently long range (i.e., comparable to the x-ray or neutron spatial coherence of the experiment), and with well-defined intermolecular separation distances. The concept of LSD has emerged quite early in the macroscopic and microscopic model formulations, in which it is usually pictured as a set of correlated like-spin adjacent molecules. Despite their success, Ising-like models are at present unable to explain the Avrami kinetics of LSD nucleation and growth derived from diffraction techniques.[38] This is well understandable since under the assumption of pseudospins on rigid-lattice sites, the Ising-like models cannot describe changes in the positions of the molecules accompanying the electronic configuration ordering and the associated local lattice distortion. Hence crystallographic LSD would not be defined. The importance of going beyond a fixed-lattice Ising model has been stressed for investigating ordering process in Cu-Au alloys[42] or lipid bilayers,[43] for instance. In the present study, the strategy for introducing magnetoelastic couplings in the Ising-like model of SC molecular solids is based on the development of the intersite (intermolecular) interactions on pairwise potentials of the Lennard-Jones (LJ) form, considering spin and lattice degrees of freedom through two coupled on-site variables, which allows for continuous molecular displacements. As a general matter of fact, these position changes are expected to highly affect the characteristics and even the nature of the transition since, even at the level of global elastic deformations coupled to a nearest-neighbor Ising model, the behavior is different from that of a rigid-lattice Ising model.[44] Our goal is to capture the essential features of the elastic contribution to the solid-state cooperativity and reconcile experimental observations derived through various techniques sensible either to the spin (spectroscopic or magnetic techniques) or the lattice variables (diffraction techniques).

The paper is organized as follows. Section II is devoted to the presentation of the Hamiltonian and the technical details of the Monte Carlo simulations. The equilibrium properties of the model are described in Sec. III, as well as the dependence of the transition mechanism (spin crossover or first-order transition) on the parameters of the model; the conditions for the presence of hysteresis are established. We finally conclude in Sec. IV.

II. MODEL AND METHOD

A. Anharmonic Ising-like model

We adopt the two-level scheme of the Ising-like model, in which the two molecular states are described by fictitious scalar spin operators σ (Fig. 1). The HS and the LS states are represented by $\sigma=+1$ and $\sigma=-1$, respectively, with corresponding g_+ and g_- degeneracies of both electronic (angular and spin) and intramolecular vibrational origins. Considering the isomorphism between this degenerate Ising-like model and the Ising model under a temperature-dependent field,[45] the on-site Hamiltonian which accounts for the inner degrees of freedom of N SC molecules is written as

$$\mathcal{H}_0 = \frac{\Delta_{\mathrm{eff}}(T)}{2}\sum_{i=1}^{N}\sigma_i, \tag{1}$$

where $\Delta_{\mathrm{eff}}(T)=\Delta-k_BT\ln(g)$ is the temperature-dependent field, with Δ as the difference in ligand-field energy between the two levels and $g=g_+/g_-\gg 1$ as the effective degeneracy ratio, related to the LS to HS electronic and vibrational entropy increase $\Delta S=k_B\ln(g)$. This two-level scheme is a drastic but appropriate simplification of the complete vibronic system.[20] The ΔS term in the effective field is the key ingredient which drives the SC process.

In the standard microscopic Ising-like model, neighboring i and j sites are coupled by a common "ferroelastic" interaction J_{ij}, irrespective of the spin states: $J_{\mathrm{HS\text{-}HS}}=J_{\mathrm{HS\text{-}LS}}=J_{\mathrm{LS\text{-}LS}}=J$. The interaction term $-J\Sigma_{i\neq j}\sigma_i\sigma_j$ is thus phenomenologically added to Eq. (1) by analogy with ferromagnetism. The thermodynamic properties of the Ising-like model are governed by the sign and temperature dependence of the effective field together with this coupling term.

Starting from the formal expression of the Ising-like model, we introduce additional degrees of freedom to ac-

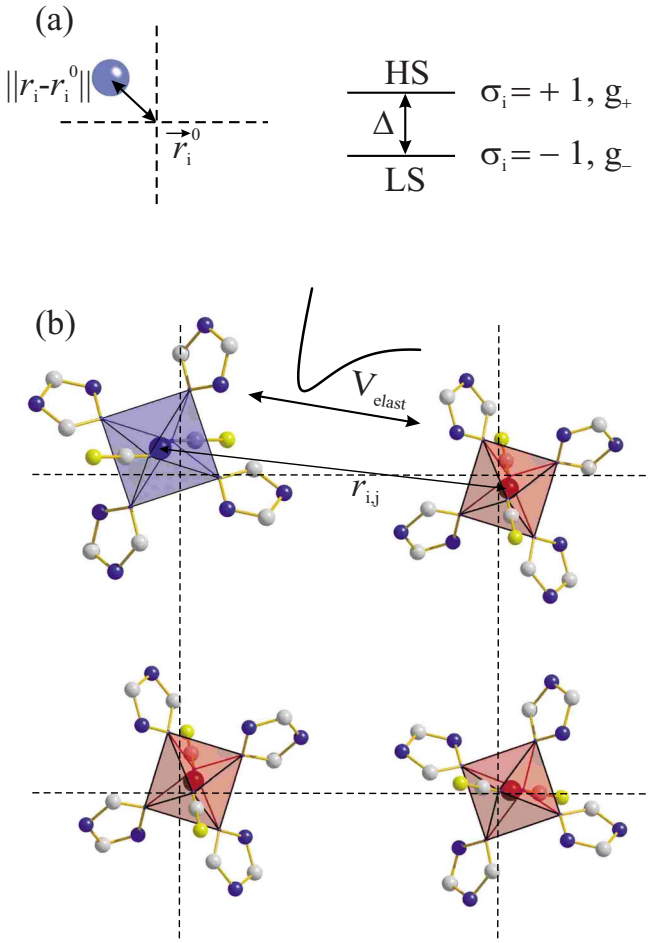

FIG. 1. (Color online) Schematic picture of the two-variable model. (a) HS molecule of spin variable σ_i at position $\vec{r}_i$, displaced from its equilibrium position $\vec{r}_i^0$. (b) Molecules on a 2D lattice with separating distance $r_{i,j}=\|\vec{r}_j-\vec{r}_i\|$ and interacting through intermolecular Lennard-Jones potentials V_{elast}.

count explicitly for the lattice energy and the local distortion (strain) of the crystal lattice, induced by a single molecule switching its spin state. Let $\vec{r}_i(x_i,y_i)$ be the instantaneous position vector of the ith site and $\vec{r}_i^0$ the equilibrium position vector in the undistorted lattice. The configuration of the system is now characterized by $3N$ variables in two dimensions $(\sigma_1,x_1,y_1,\ldots,\sigma_i,x_i,y_i,\ldots,\sigma_N,x_N,y_N)$. The interaction energy can be written in the general form as a lattice sum:

$$\mathcal{H}_{\text{lat}}(\{\sigma\},\{\vec{r}\}) = \sum_{\langle i,j\rangle} A(\sigma_i,\sigma_j) V_{\text{elast}}(r_{\langle i,j\rangle}, r^0_{\langle i,j\rangle}), \tag{2}$$

where the sum runs over all nearest-neighbor pairs $\langle i,j\rangle$. $r_{\langle i,j\rangle}=\|\vec{r}_j-\vec{r}_i\|$ and $r^0_{\langle i,j\rangle}=\|\vec{r}_j^0-\vec{r}_i^0\|$ are the neighboring intersite instantaneous distance and equilibrium distance, respectively. The interaction energy depends therefore only on the local environment of each independent molecule, such as the distribution of other molecules and their distance to it, as well as their spin state [Fig. 1(b)]; this is at variance with the standard Ising-like model. In another context, it has been formulated in a similar way for modeling magneto-elastic couplings in three-dimensional (3D) Ising schemes.[46–48] An important issue is that the intersite distance corresponds to the Fe···Fe separation, as illustrated in Fig. 1, and should not be confused with the true intermolecular distances usually characterized from structural analyses (e.g., H···O hydrogen bonds and C···C short contacts).

In some cases, it has been recognized that in addition to the electronic and intramolecular vibrational entropy changes, the latter being mostly related to the Fe-N stretching and octahedron distortion modes, intermolecular (lattice) vibrations may also contribute significantly.[49] Zimmermann and Konig[50] applied a simple Debye model with two different Debye temperatures (Θ_{HS} and Θ_{LS}) to account for the entire vibrational contribution. From accurate single-crystal diffraction measurements, we have concluded that the 2D polymeric SC compound $[\text{Fe(btr)}_2(\text{NCS})_2]\cdot\text{H}_2\text{O}$ exhibits lattice modes of higher vibration amplitudes in the HS state. Related to this, the HS and LS crystal lattices exhibit a different thermal-expansion behavior.[51] The thermoelastic properties for such SC systems is obviously dependent on the spin state, and therefore has to be considered in the model. As a consequence, the independence of the interaction parameter J with the spin state in the standard Ising-like model is a drastic approximation, which we relax here. The equilibrium distance $r^0_{\langle i,j\rangle}$ in the undistorted lattice and the elastic coupling $A(\sigma_i,\sigma_j)$ between a pair of molecules i and j are considered as follows:

$$\begin{aligned} A(\sigma_i,\sigma_j) &= A_{\text{HS}} \quad r^0_{\langle i,j\rangle} = r_{\text{HS}} \quad \text{if} \quad \sigma_i=\sigma_j=1, \\ &= A_{\text{HL}} \qquad = r_{\text{HL}} \quad \text{if} \quad \sigma_i=-\sigma_j, \\ &= A_{\text{LS}} \qquad = r_{\text{LS}} \quad \text{if} \quad \sigma_i=\sigma_j=-1. \end{aligned} \tag{3}$$

The intersite equilibrium distances correspond to the intermolecular distances in the HS and LS phases (called lattice spacing for simplicity hereafter). We recall that they are not relative to the internal Fe-N distance. Although the intermolecular distances are known to be different in the HS and LS phases, typical values cannot be given *a priori*.

Condition (3) can be formally rearranged to

$$A(\sigma_i,\sigma_j) = J_0 + J_1(\sigma_i+\sigma_j) + J_2\sigma_i\sigma_j, \tag{4}$$

with

$$J_0 = \frac{(A_{\text{HS}} + 2A_{\text{HL}} + A_{\text{LS}})}{4},$$

$$J_1 = \frac{(A_{\text{HS}} - A_{\text{LS}})}{4},$$

$$J_2 = \frac{(A_{\text{HS}} - 2A_{\text{HL}} + A_{\text{LS}})}{4}. \tag{5}$$

A relation similar to Eq. (4) was derived separately by Bolvin and Kahn[28] and Boukheddaden *et al.*[32] In our case, V_{elast} in Eq. (2) takes the form of an anharmonic intersite potential of the empirical (6-3) LJ form with finite range r_{max}:

$$\text{(i) if } r_{\langle i,j\rangle} \le r_{\text{max}}$$

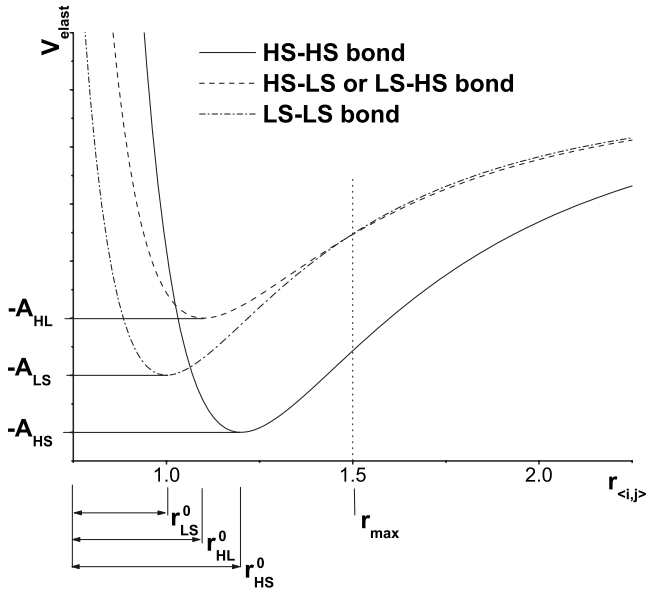

FIG. 2. Spin-dependent Lennard-Jones potentials $A(\sigma_i,\sigma_j)V_{\text{elast}}$ describing elastic interactions between two nearest-neighbor sites i and j. The position and depth of the potentials define three lattice spacings $(r^0_{\text{HS}},r^0_{\text{HL}},r^0_{\text{LS}})$ and three intermolecular couplings $(A_{\text{HS}},A_{\text{HL}},A_{\text{LS}})$. $r_{\max}$ is specified as a vertical dotted line.

$$V_{\text{elast}}(r_{\langle i,j\rangle},r^0_{\langle i,j\rangle}) = \left(\frac{r^0_{\langle i,j\rangle}}{r_{\langle i,j\rangle}}\right)^6 - 2\left(\frac{r^0_{\langle i,j\rangle}}{r_{\langle i,j\rangle}}\right)^3,$$

(ii) if $r_{\langle i,j\rangle} > r_{\max}$

$$V_{\text{elast}}(r_{\langle i,j\rangle},r^0_{\langle i,j\rangle}) = 0. \tag{6}$$

The first term in V_{elast} results from strong short-range repulsive interaction, while the second term represents the long-range attractive interaction. V_{elast} is a dimensionless quantity; the real elastic interaction is given by $A(\sigma_i,\sigma_j)V_{\text{elast}}$, as specified in Eq. (2). The choice of $r_{\max}$ is crucial to ensure the stability of the crystal lattice and retain the structural topology (each site surrounded by four neighbors on the square lattice). In other words, there is no diffusion of molecules across the whole system. It is to be noted that $r_{\max}$ prevents the algorithm from accessing the entire phase space spanned by the translational degrees of freedom. Three different potentials are considered for HS-HS, HS-LS, and LS-LS neighboring pairs (Fig. 2). The position of the minimum is relative to the corresponding equilibrium distance r^0_{HS}, r^0_{HL}, r^0_{LS}, defining three lattice spacings. The potential depth is related to the strength of the intermolecular coupling A_{HS}, A_{HL}, A_{LS}. For all the simulations, the equilibrium distances of the undistorted lattices take the values $r^0_{\text{HS}}=1.2$, $r^0_{\text{HL}}=1.1$, and $r^0_{\text{LS}}=1$, which correspond to a more compact LS phase; this is the experimentally observed usual trend. Intersite equilibrium distances between LS and HS species are intermediate between purely LS and HS ones. These chosen values for the equilibrium distances are not relative to any specific compound, but exaggerated to amplify the effects. The essential characteristic of the selected LJ potential is the asymmetry, leading to the desired anharmonicity. In a first approximation, harmonic potentials can successfully predict many properties of the solid. However, anharmonic terms in the intermolecular potentials are responsible for several phenomena, important in the context of SC, such as thermal expansion, compressibility, and thermal conductivity. The chosen parameters of the LJ potentials ensure a stiffer lattice in the LS state with respect to the HS state, and correspond to a lower bulk modulus B in the HS state. B is related to the second derivative of the crystal energy with respect to the volume. In the case of pairwise additive central intermolecular potentials, B is given by the second derivative of the potential with respect to the intersite distance. Considering our scheme, B for the pure HS or LS lattices is roughly related to the curvatures of the LJ potentials at the equilibrium HS and LS distances. It is less straightforward for the intermediate-spin configurations. It is clear from Fig. 2 that the curvature is more pronounced in the LS state. For quantitative confrontation with experimental data, a more efficient intermolecular force field would be more appropriate, possibly of the Buckingham exp-6 form, augmented with electrostatic interactions through distributed multipole expansions.[52] The optimum parameters of the LJ potentials could be determined through an appropriate optimization procedure by the knowledge of the cohesive crystal energy, lattice parameters, and thermal-expansion tensors of the HS and LS pure phases.[53]

The total two-variable Hamiltonian $\mathcal{H}(\{\sigma\},\{\vec{r}\})$ can finally be written as

$$\mathcal{H}(\{\sigma\},\{\vec{r}\}) = \sum_{\langle i,j\rangle} V_{\text{elast}}(r_{\langle i,j\rangle},r^0_{\langle i,j\rangle})\{J_0 + J_1(\sigma_i+\sigma_j) + J_2\sigma_i\sigma_j\} + \frac{\Delta_{\text{eff}}}{2}\sum_i \sigma_i, \tag{7}$$

where J_0V_{elast} takes only negative values, whereas J_1V_{elast} and J_2V_{elast} may be either positive or negative, depending on the respective depth of the LJ potentials. When $J_2V_{\text{elast}}<0$, the system is ferroelastic, while for $J_2V_{\text{elast}}>0$, the system is said to be antiferroelastic. Although ferroelastic materials is the general case, a few examples of the second kind have been discovered so far.[54] This expression of the interaction energy as the sum of three terms is similar to a formulation of Ising-like model based on elasticity theory,[32,55] although for the latter, the interaction energy is identical for HS-HS and LS-LS pairs and the corresponding J_0 term is a constant energy shift. We chose here the cohesive energy of the pure HS and LS phases as different, which is rationalized by the fact that both phases usually exhibit modifications of the supramolecular organization, even possibly related to a space-group change (crystallographic phase transition). Contrasting with the standard Ising-like model, the LJ pair potentials lead to coupling parameters which are defined locally and depend on the pair $\langle i,j\rangle$. The entire system exhibits therefore a distribution of interaction constants. A similar idea has also been introduced in a thermodynamic model to explain unusual spin transition features.[56] The introduction of lattice degrees of freedom allows the couplings to fluctuate when the system is in contact with a thermal bath, which

we consider in the following. The system can be characterized by two quantities: the magnetization per site $\langle\sigma\rangle$ and the mean intersite distance $\langle r\rangle$ (lattice spacing) defined as

$$\langle\sigma\rangle = \frac{1}{\mathcal{Z}}\sum_{\{\sigma\}}\left\{\sum_{i=1}^{N}\frac{\sigma_i}{N}\right\}\int_{\Re}\prod_{k=1}^{N}d\vec{r}_k\exp(-\beta\mathcal{H}), \tag{8}$$

$$\langle r\rangle = \frac{1}{\mathcal{Z}}\sum_{\{\sigma\}}\int_{\Re}\prod_{k}^{N}d\vec{r}_k\left\{\sum_{\langle i,j\rangle}^{M}\frac{r_{\langle i,j\rangle}}{M}\right\}\exp(-\beta\mathcal{H}), \tag{9}$$

where $\Sigma_{\{\sigma\}}=\Sigma_{\{\sigma_1\}}\times\cdots\times\Sigma_{\{\sigma_N\}}$ corresponds to a sum over all spin configurations and $\int_{\Re}\Pi_{k=1}^{N}d\vec{r}_k=\int_{-\infty}^{\infty}d\vec{r}_1\times\cdots\times\int_{-\infty}^{\infty}d\vec{r}_N$ to a continuous sum over all position vector configurations accessible for the system. $\mathcal{Z}=\Sigma_{\{\sigma\}}\int_{\Re}\Pi_{i=1}^{N}d\vec{r}_i\exp(-\beta\mathcal{H})$ is the canonical partition function and $\exp(-\beta\mathcal{H})$ is the Boltzmann weight with $\beta=1/k_BT$ corresponding to the inverse temperature ($k_B=1$). M is the number of intersite bonds.

B. Dynamical aspects and Monte Carlo simulations

In order to study the static properties of Hamiltonian (7), we perform MC simulations on a simple square deformable lattice with free boundary conditions. We adopt the *NVT*-MC method, where N is the number of sites (molecules), V is the volume of the system, and T is the thermal bath temperature. The use of periodic conditions would have required a treatment in the isobaric (N,P,T) statistical ensemble, where P is the pressure of the system, allowing the area of the system to fluctuate through a length rescaling. Let $\mathcal{P}(\sigma_1,\ldots,\sigma_N,\vec{r}_1,\ldots,\vec{r}_N,t)$ be the probability for the system to have the spin configuration $(\sigma_1,\ldots,\sigma_N)$ and the position vector configuration $(\vec{r}_1,\ldots,\vec{r}_N)$ at Monte Carlo step (MCS) t. We assume that the $\mathcal{P}(\{\sigma\},\{\vec{r}\},t)$ evolution is governed by the master equation

$$\mathcal{P}(\{\sigma\},\{\vec{r}\},t+1) = \int\prod_{i=1}^{N}d\vec{r}_i'^{N}\sum_{\{\sigma'\}}\Omega(\{\sigma'\},\{\vec{r}'\}\rightarrow\{\sigma\},\{\vec{r}\})\mathcal{P}(\{\sigma'\},\{\vec{r}'\},t)-\Omega(\{\sigma\},\{\vec{r}\}\rightarrow\{\sigma'\},\{\vec{r}'\})\mathcal{P}(\{\sigma\},\{\vec{r}\},t), \tag{10}$$

where $\Omega(\{\sigma\},\{\vec{r}\}\rightarrow\{\sigma'\},\{\vec{r}'\})$ is the transition rate corresponding to the conditional probability for the system to have the $(\{\sigma'\},\{\vec{r}'\})$ configuration at MCS t knowing it was $(\{\sigma\},\{\vec{r}\})$ at MCS $t-1$. The transition probability is imposed to follow the Boltzmann equilibrium distribution. The stationary condition $\partial\mathcal{P}(\{\sigma\},\{\vec{r}\},t)/\partial t=0$ leads to the well-known necessary but nonsufficient detailed balance condition

$$\frac{\Omega(\{\sigma'\},\{\vec{r}'\}\rightarrow\{\sigma\},\{\vec{r}\})}{\Omega(\{\sigma\},\{\vec{r}\}\rightarrow\{\sigma'\},\{\vec{r}'\})}=\frac{\exp[-\beta\mathcal{H}(\{\sigma\},\{\vec{r}\})]}{\exp[-\beta\mathcal{H}(\{\sigma'\},\{\vec{r}'\})]}. \tag{11}$$

In the following, we choose two transition probabilities, $W_{\mathrm{spin}}(\{\sigma'\}\rightarrow\{\sigma\})$ for the spin variables and $W_{\mathrm{elast}}(\{\vec{r}'\}\rightarrow\{\vec{r}\})$ for the displacement vectors, which is justified by the different characteristic time at which electronic and lattice deformation processes in the adiabatic approximation take place. As a matter of fact, electron transitions occur within femtoseconds, while atomic displacement and vibrational relaxation occur in the picosecond to nanosecond time scale. A nonconserved order-parameter dynamic is chosen for $W_{\mathrm{spin}}(\{\sigma'\}\rightarrow\{\sigma\})$ and $W_{\mathrm{elast}}(\{\vec{r}'\}\rightarrow\{\vec{r}\})$. For dealing with the nonequilibrium behavior of the SC phenomenon, the appropriate choice of the transition rate would be of Arrhenius type, which allows one to correctly reproduce the sigmoidal relaxation curves of the HS fraction at very low temperature.[21,22,27] In the present case, we restrict the analysis to the equilibrium properties of our model; the nonequilibrium study will be the subject of a future publication. We choose the Metropolis single-variable-changing dynamics[57] for the two variables of the Hamiltonian. The different sequences of a MCS are as follows: (i) A lattice site i is chosen randomly and the fictitious spin σ_i flip is updated according to the Metropolis acceptance criterion. (ii) Another site j at the position $\vec{r}_j(x_j,y_j)$ is chosen randomly and a new position $\vec{r}_j'(x_j',y_j')$ is proposed as

$$x_j' = x_j + d_{x_j},$$

$$y_j' = y_j + d_{y_j}, \tag{12}$$

where d_{x_j} and d_{y_j} are random continuous displacements drawn on a Gaussian distribution of zero mean and adjustable variance. The new position of the site is evaluated and updated using the Metropolis scheme. (iii) The two previous stages are repeated N times. The spin and lattice variables are thus technically decoupled in the algorithm; the real interplay comes from the Hamiltonian. MC simulations have been performed on 32×32 square lattice ($N=1024$) with open boundary conditions. In addition, for simplicity, J_1 has been set to 0 in all calculations, corresponding to A_{LS} being equal to A_{HS}. Although this assumption simplifies our Hamiltonian, this does not bring a real severe limitation since J_1 mostly affects the transition temperature (*vide supra*).

III. EQUILIBRIUM BEHAVIOR OF THE ANHARMONIC MODEL

The properties of the model defined by Hamiltonian (7), called hereafter as anharmonic model, are described according to the behavior of the intrinsic parameters n_{HS} and $r_{\langle i,j\rangle}^{\mathrm{norm}}$. n_{HS} can be defined as a function of the fictitious magnetization:

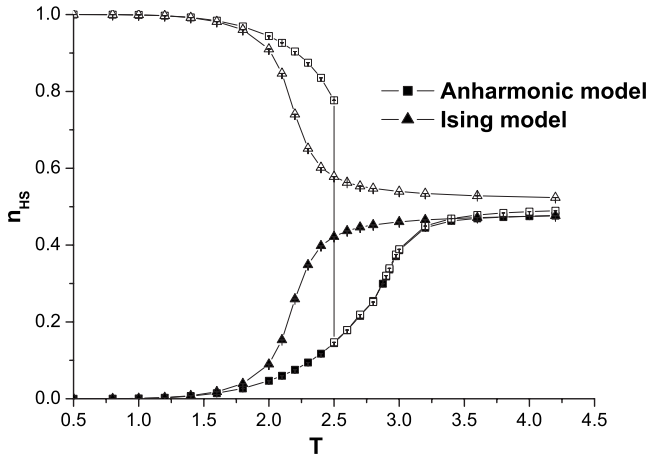

FIG. 3. Temperature dependences of n_{HS} for the anharmonic (squares) and zero-field finite-size Ising model (triangles). Systems prepared in ordered (HS) and (LS) phases are represented by open and filled symbols, respectively. Parameters of the model: $J_0=999$, $J_1=0$, and $J_2=1$.

$$n_{\mathrm{HS}} = \frac{1+\langle\sigma\rangle}{2}. \tag{13}$$

The dimensionless and normalized lattice spacing $r^{\mathrm{norm}}_{\langle i,j\rangle}$ is relative to the distance between two neighboring sites i and j. Its thermodynamic average r^{norm} is given by

$$r^{\mathrm{norm}} = \frac{\langle r\rangle - r^0_{\mathrm{LS}}}{r^0_{\mathrm{HS}} - r^0_{\mathrm{LS}}}, \tag{14}$$

where $\langle r\rangle$ is the average intersite distance in the system.

A. $\Delta_{\mathrm{eff}}=0$ case

We discuss in a first step the behavior of the anharmonic model without effective field and setting $J_1=0$, and interpret it with respect to the phase diagram of the well-known zero-field Ising model defined by

$$\mathcal{H}_{\mathrm{Ising}} = -J_2 \sum_{\langle i,j\rangle} \sigma_i\sigma_j, \tag{15}$$

where J_2 is the usual coupling constant. Both models (anharmonic and zero-field Ising model) have been treated using identical system size to have an estimate of finite-size effects, the true Curie temperature of the 2D Ising model at the thermodynamic limit being indeed well known.[58] The phase diagram is derived using the following procedure. At $t=0$ the system is prepared in a totally ordered HS ($n_{\mathrm{HS}}=r^{\mathrm{norm}}=1$) or LS ($n_{\mathrm{HS}}=r^{\mathrm{norm}}=0$) configuration. For $t>0$ the system is in contact with a thermal bath at a temperature T. The observables n_{HS} and r^{norm} are estimated as the average over 6×10^5 MCSs, using only configurations after a waiting time τ_w (i.e., disregarding configurations in the nonequilibrium transient regime). For the different simulations, τ_w range from 10^4 to 10^5 MCSs per spin for temperatures far from and near the critical point, respectively. The results are given in Fig. 3.

Just as the Ising case, the anharmonic model presents a disordered ($n_{\mathrm{HS}}=1/2$) phase at high temperature and an ordered phase ($n_{\mathrm{HS}}\neq 1/2$) at low temperature, separated by a critical temperature T_C not estimated in this work.[59] It is well known that in the ordered phase, the free-energy density of the Ising model $f_{\mathrm{Ising}}(n_{\mathrm{HS}})$ has two symmetric and degenerate stable solutions $n^0_{\mathrm{HS+}}(T)$ and $n^0_{\mathrm{HS-}}(T)$ for $\Delta_{\mathrm{eff}}\to 0_+$ and $\Delta_{\mathrm{eff}}\to 0_-$, respectively, surrounding the unstable solution $n_{\mathrm{HS}}=1/2$. Obviously, it is expected that the application of a nonzero field Δ_{eff} would break the symmetry between $n^0_{\mathrm{HS+}}$ and $n^0_{\mathrm{HS-}}$. Surprisingly, even if the temperature-dependent field Δ_{eff} is absent, the anharmonic model does not have this symmetry between the two states. This is due to the deliberate choice of different LJ potentials for HS and LS states [Eq. (6)], which corresponds to an additional entropy difference δS_{add} between the HS and the LS phases. δS_{add} acts as an additional field, noted as $\tilde{h}$, which breaks the symmetry between the two states in the free-energy density $f(n_{\mathrm{HS}})$, as schematically represented in Fig. 4. This additional field is a key feature of this anharmonic model. Under such conditions, the overall effective field $(\Delta_{\mathrm{eff}}+\tilde{h})$ cannot be easily canceled since $V_{\mathrm{elast}}(r_{\langle i,j\rangle}, r^0_{\langle i,j\rangle})$ itself depends on the spins σ_i and σ_j due to the fact that $r^0_{\langle i,j\rangle}$ depends on the spin values of the sites i and j. Figure 3 indicates that the more compact $n^0_{\mathrm{HS-}}(T)$ phase is the stable one, while $n^0_{\mathrm{HS+}}(T)$ is metastable. The additional entropy term can be formally written as additional degeneracies, originating from lattice vibrations (phonons), as will be shown by solving analytically Hamiltonian (7) in a forthcoming paper. For a purely harmonic 1D SC chain, the corresponding degeneracy is simply related to the ratio of LS and HS elastic constants.[32] A similar dependence on A_{LS} and A_{HS}, but a more complicated one, does exist for the present anharmonic model.

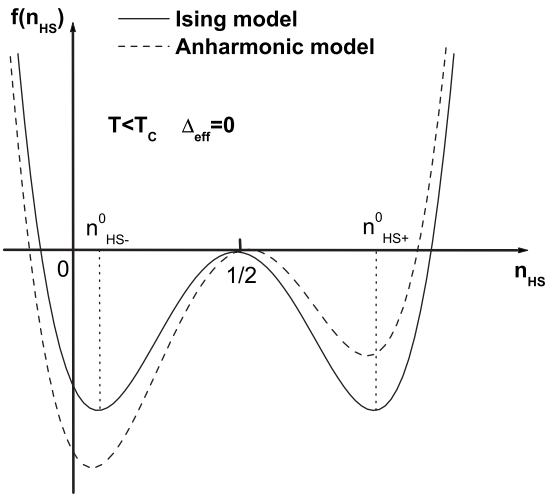

FIG. 4. Schematic representation of the free-energy density $f(n_{\mathrm{HS}})$ in the ordered phase ($T<T_C$) for the zero-field Ising (full line) and the anharmonic (dotted line) model with $\Delta_{\mathrm{eff}}(T)=0$.

B. $\Delta_{\mathrm{eff}}\neq 0$ case

We now study the $\Delta_{\mathrm{eff}}\neq 0$ case, setting $\ln(g_+/g_-)=4$ for all MC simulations. The two-dimensional Ising-like model under temperature-dependent field has been widely studied numerically[24] and exactly in the mean-field approximation.[21]

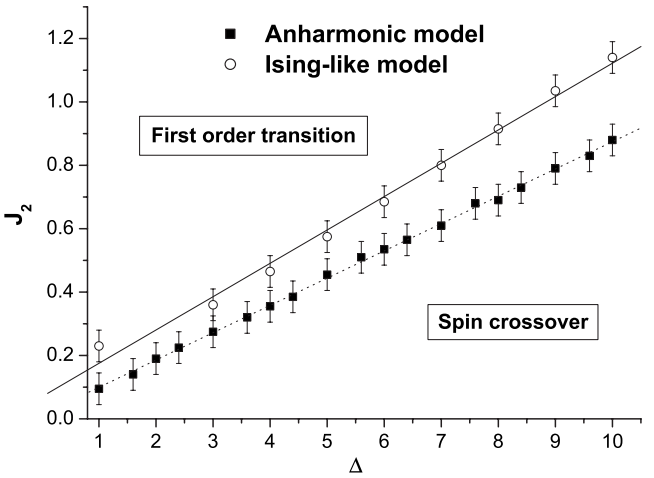

FIG. 5. J_2-Δ phase diagram of the anharmonic (filled squares) and finite-size Ising-like models (open circles) (J_0=999 and J_1=0).

Following previous treatment, the corresponding transition temperature T_{equ}, at which $\langle\sigma\rangle=0$ and $n_{HS}=1/2$, is defined by the condition

$$\Delta_{eff} = \Delta - k_B T_{equ} \ln(g) = 0, \tag{16}$$

which gives

$$T_{equ} = \frac{\Delta}{k_B \ln(g)}. \tag{17}$$

This definition of T_{equ} is an approximation; the true transition temperature corresponds to the temperature at which the free energies of the HS and LS states are equal. However, MC simulations do not allow the determination of the free energy of the system, which justifies the use of this approximation. For the Ising-like model, the equilibrium temperature is known to be independent of the coupling parameter J_2 [see Eq. (17)], while the sharpness of the spin transition increases with J_2. Whether the change in n_{HS} is continuous (gradual) or discontinuous (first-order character) depends on whether T_{equ} is above or below the critical temperature of the corresponding zero field Ising model T_{Ising}.[58] The transition line between spin crossover and first-order transition in the J_2-Δ phase diagram of the anharmonic model has been determined in the following way. Thermal hysteresis loops have been performed by varying J_2 parameters for different fixed Δ values until the total disappearance of bistability is observed, which corresponds to the transition line. As seen in Fig. 5, the anharmonic model displays such a critical behavior but the transition line differs from the finite-size Ising-like model. This suggests that the critical temperature T_C of the anharmonic model is different from that of the simple Ising case. The introduction of the anharmonic coupling favors the first-order transition behavior. In agreement with our findings, it has been shown that the introduction of anharmonic contribution to the 1D atom-phonon model sharpens also the spin transition and drives the "first-order" character.[33] As expected, first-order character is observed for high J_2 values and weak HS to LS ligand-field energy difference Δ.

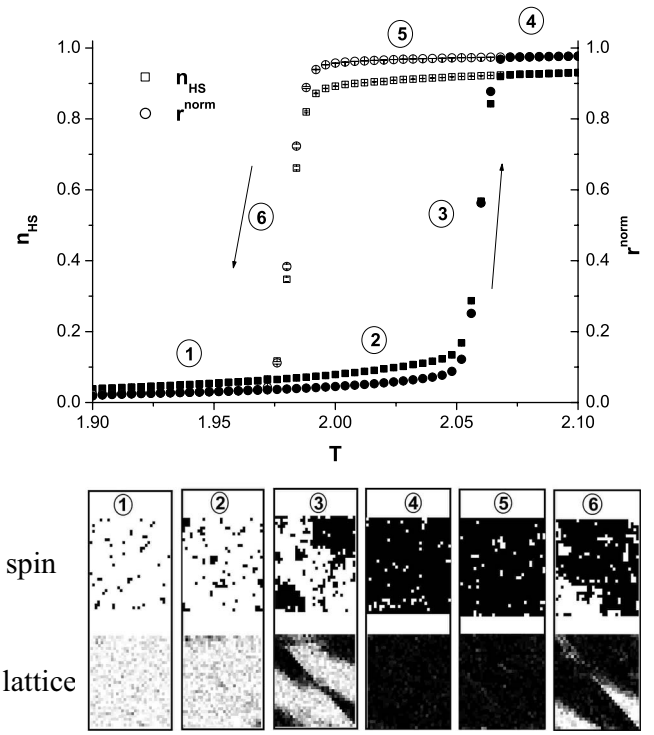

FIG. 6. Top: Temperature dependences of n_{HS} (squares) and r^{norm} (circles) in the anharmonic model with J_0=999, J_1=0, and Δ=8. J_2 has been chosen above the transition line defined in Fig. 5 such as J_2=0.9. The two observables are reported during the warming (filled symbols) and cooling modes (open symbols). Bottom: Snapshots of the configuration of the system at different temperatures in the hysteresis loop. Spin [black: (HS) state; white: (LS) state] and lattice (black: $r^{norm}_{\langle i,j\rangle}=r^0_{HS}$; white: $r^{norm}_{\langle i,j\rangle}=r^0_{LS}$; shaded gray: $r^0_{LS}<r^{norm}_{\langle i,j\rangle}<r^0_{HS}$) observables are represented on top and bottom, respectively. The thermal loops have been performed using 2000 Monte Carlo transient steps at a heating rate of $dT/dt=2\times10^{-6}$ K MCS^{-1} in the warming and then cooling modes, the initial system configuration being the final configuration of the previous temperature. Error bars are smaller than the symbols.

The two extreme cases, namely, those of first-order thermal spin transition and simple spin crossover, are represented in Figs. 6 and 7, respectively. Figure 6 shows an abrupt transition with hysteresis. Snapshots of the configuration of the system at several temperatures display the different stages of the LS→HS and HS→LS phase transformations. The (1) and (2) [(4) and (5)] upper snapshots show germ nucleation of the HS (LS) state within the LS (HS) phase. The (3) and (6) upper snapshots present LS and HS coarsening spin domains. Our two-variable model allows also probing the corresponding configuration of the crystal lattice. On the lower snapshots in Fig. 6, equilibrium distances in the undistorted LS and HS lattices are represented in white and black, respectively, while intermediate distances are represented in grayscale. Each thermally induced germ nucleation leads to a local lattice distortion, which grows to a structurally defined domain of large area [lower snapshots (3) and (6)]. These coarsening domains coexist in the system near T_{equ}: the transition is heterogeneous with structural phase separation. The separation between HS and LS domains is clearly not abrupt,

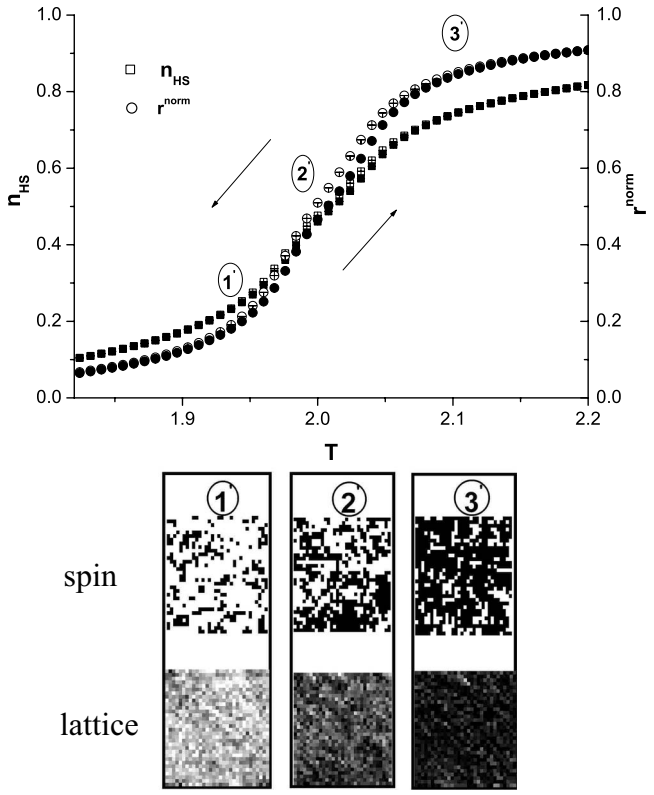

FIG. 7. Top: Temperature dependences of n_{HS} (squares) and r^{norm} (circles) in the anharmonic model with $J_0=999$, $J_1=0$, and $\Delta=8$, computed as in Fig. 6. J_2 has been chosen below the transition line defined in Fig. 5 such as $J_2=0.6$. Bottom: Snapshots of the configuration of the system as in Fig. 6.

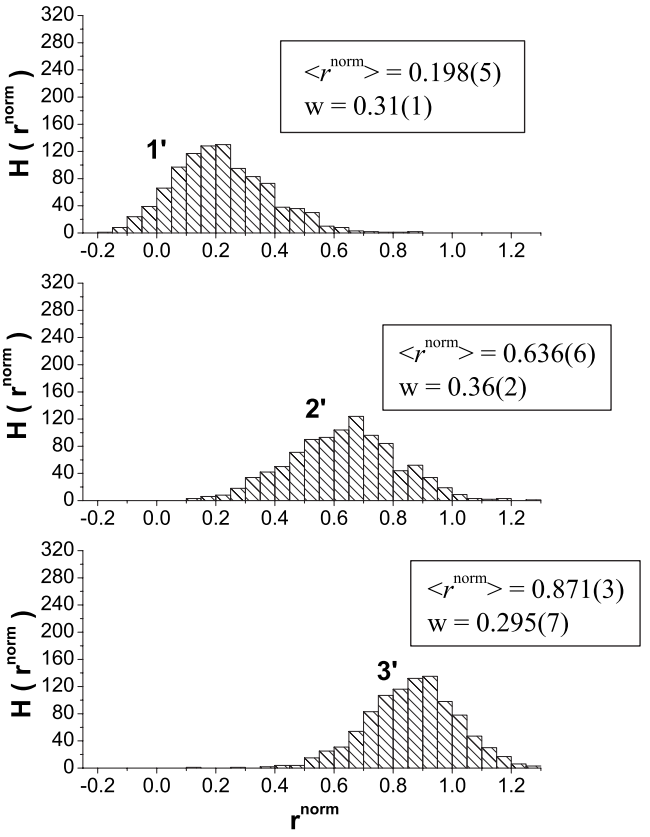

FIG. 8. Distributions of intersite distance $H(r^{norm}_{\langle i,j\rangle})$ corresponding to a gradual spin conversion, relative to snapshots 1′, 2′, and 3′ in Fig. 7. The inset gives the mean value $\langle r^{norm}\rangle$ and width w of each distribution.

owing to the continuous character of the lattice variable; relaxation of the lattice spacing occurs, which corresponds to domain walls. Such a behavior is obviously not accessible in a rigid-lattice model such as the standard Ising-like one. This domain structure is expected for a first-order transition, due to the short-range nature of the interactions in our model. The usual short-range Ising model itself presents such a characteristic clustering. Our results can be related and compared to the elastic Ising-like model of Konishi *et al.*[36] and Miyashita *et al.*,[37] in which the interactions are developed on a purely harmonic intersite potential, furthermore identical for HS and LS. This latter restriction is dissimilar to our scheme and leads to a mean-field behavior (no short-range interactions).[37] This harmonic elastic model does not exhibit cluster growth, and accordingly cannot explain phase-separation effects, as evidenced by diffraction techniques.[38–41]

In the same way, the case of thermal spin crossover has been investigated (Fig. 7). No metastable state exists; the process is dominated by nucleation leading to a gradual conversion without hysteresis. All along the transition, the lattice spacing is intermediate between the equilibrium distances in the HS and LS undistorted phases; the transition is homogeneous. Structural relaxation spreads the whole system. In addition, the lattice spacing directly follows the fraction of HS species; in other words, the Végard law is satisfied.

r^{norm} is a simplistic descriptor for how the crystal lattice reacts to the spin conversion; the analysis of the distribution of the $r^{norm}_{\langle i,j\rangle}$ distances is more informative. It is represented in the form of histograms $H(r^{norm}_{\langle i,j\rangle})$ in Figs. 8 and 9, corresponding respectively to the $J_2=0.6$ and $J_2=0.9$ cases discussed above.

In the case of a spin crossover (Fig. 8), the distribution consists of a large single peak whatever the temperature is, which corresponds to a gradual change in the lattice spacing in the crystal. This is related to a homogeneous transformation mechanism without crystallographic phase separation. One can notice that the distribution of lattice spacing is quite dispersed around the mean value. This is typical for a gradual spin conversion in our model and is attributed to weak intermolecular couplings. Starting from the LS state and increasing the temperature, the width of the distribution first increases as the spin conversion proceeds, as a consequence of increased lattice distortions. In the late steps of the conversion, the distribution finally becomes narrower. Distributions 1, 3, and 4 (Fig. 9) present a radically different behavior for the first-order transition case. At low temperature (histogram 1), a sharp single peak centered around the lattice spacing of the LS undistorted phase ($r^{norm}=0$) is observed. As temperature increases in the bistability area (hysteresis loop), a second peak appears centered around the HS lattice parameter ($r^{norm}=1$). The double peak evidences domain formation with phase coexistence (the metastable and the thermodynamically stable phases) separated by domain walls. At the same time, both distributions widen, as a consequence of

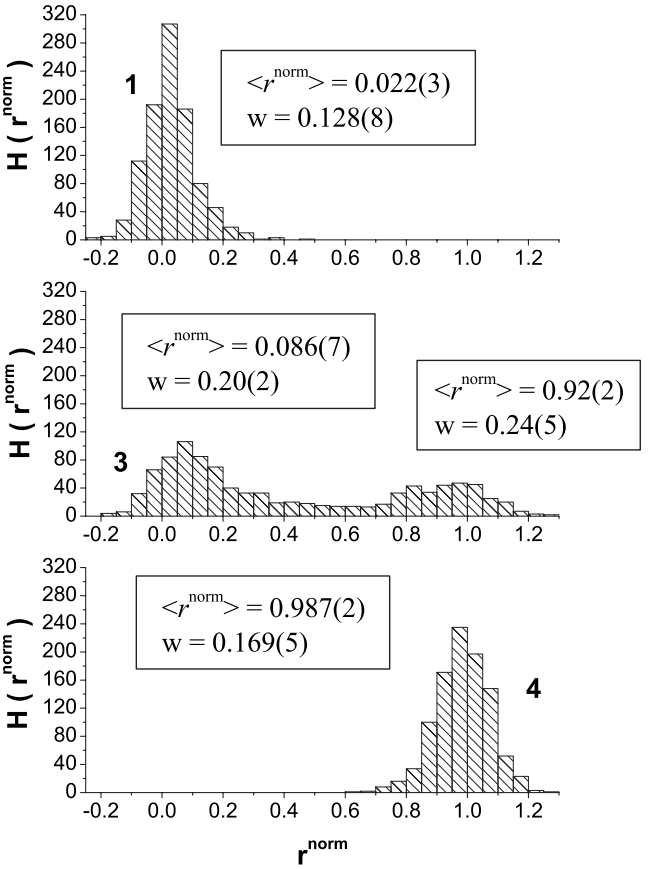

FIG. 9. Distributions of intersite distance $H(r^{\mathrm{norm}}_{\langle i,j\rangle})$ in the case of first-order transition, relative to snapshots 1, 3, and 4 in Fig. 6 in the warming process. The inset gives the mean value $\langle r^{\mathrm{norm}}\rangle$ and width w of each distribution.

structural relaxation, at the domain walls principally. In the final step of the transition, the ($r^{\mathrm{norm}}=1$) peak sharpens and long-range order is restored in the HS phase. It is noteworthy that distributions 2′ and 3 correspond to a quite similar HS fraction but exhibit radically different behaviors. This difference can be related to the observations reported in the literature from x-ray- and neutron-diffraction measurements. In the case of highly cooperative materials, the diffraction pattern usually consists of a superposition of the diffraction patterns of the LS and HS phases, with Bragg-peak splitting. This has been attributed to phase coexistence in the bistability region.[38–41] On the contrary, for a homogeneous transition, a continuous peak displacement occurs.[60]

It is noteworthy that owing to the asymmetric (anharmonic) form of the intermolecular LJ potentials, the model specifically accounts for the thermal expansion of the crystal lattice as illustrated in Fig. 10. For this simulation, the spin configuration for all the sites of the system has been fixed to HS or LS (bypassing the spin Metropolis update in the algorithm). Only the lattice variables were allowed to change. The mean lattice spacing has been evaluated as a function of temperature. As temperature increases, thermal fluctuations lead to a higher probability for $\langle r\rangle$ to be greater than r^0_{HS} and r^0_{LS} in the HS and LS states, respectively. This directly results from the repulsive contribution of the LJ potential being much stronger than the attractive part (see Fig. 2). In agreement with the chosen shape of the LJ potentials, the derived linear thermal-expansion coefficient is higher in the HS state than in LS.

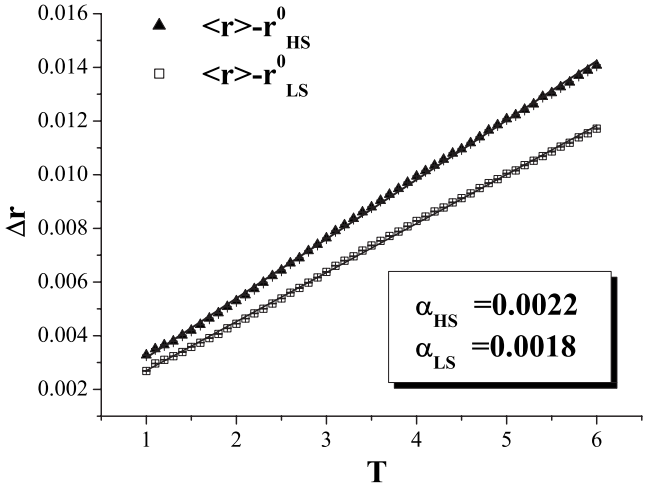

FIG. 10. Temperature dependences of the mean lattice spacing $\langle r\rangle$ for the pure LS and HS phases (i.e., in the absence of spin conversion). The linear thermal-expansion coefficients α have been fitted by straight lines. The HS and LS corresponding values are given in the inset.

C. Condition for the presence of hysteresis

In this section, we analyze the dependence of the equilibrium temperature T_{equ} and hysteresis width δT as a function of the parameters J_0, J_1, and J_2 of the anharmonic model. For the standard Ising-like model (with z neighbors), it has been shown from a mean-field treatment that the condition for hysteresis (bistability) is simply given by

$$zJ_2 > \frac{\Delta}{\ln g}. \tag{18}$$

When J_2 is large compared to Δ, the change in n_{HS} is discontinuous and the LS→HS conversion corresponds to a first-order transition. Conversely, when J_2 is small compared to Δ, the change in n_{HS} is gradual, as is the case for a spin crossover. The steepness of the change in n_{HS} at T_{equ} depends on the amplitude of J_2, the transition becoming more abrupt for large J_2.

In the case of the anharmonic model, we have noted in Sec. II that the spin dependence of the LJ potentials behaves as an additional phonon contribution $\tilde{h}$ to the temperature-dependent field Δ_{eff}. This suggests a nontrivial dependence of T_{equ} and δT on the parameters J_0, J_1, and J_2. In the following, we restrict the discussion to the more informative case of highly cooperative system undergoing a first-order transition. T_{equ} and δT are defined as follows:

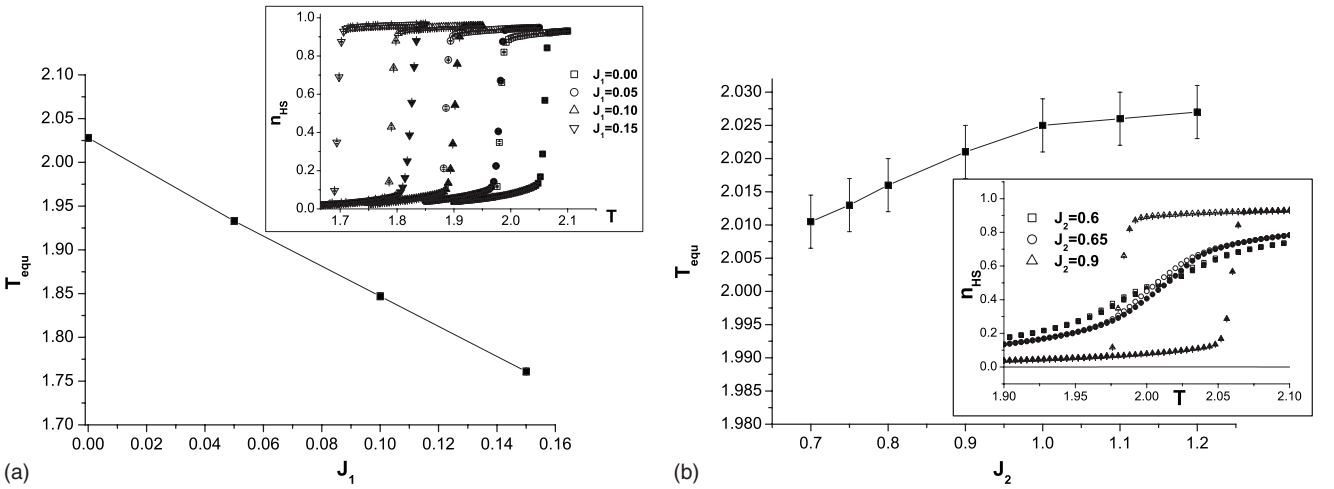

FIG. 11. Variations in equilibrium temperature T_{equ} for $\Delta=8$: (a) with J_1 ($J_0=1000$ and $J_2=0.9$) and (b) with J_2 ($J_0=999$ and $J_1=0$). Insets in each plot correspond to thermal hysteresis loops when (a) J_1 and (b) J_2 vary. ($J_2=0.65$ corresponds approximately to the critical point at which the hysteresis loop opens.)

$$T_{equ} = \frac{T_{\uparrow} + T_{\downarrow}}{2},$$

$$\delta T = T_{\uparrow} - T_{\downarrow}, \tag{19}$$

where $T_{\uparrow}$ and $T_{\downarrow}$ are spin transition temperatures in the warming and cooling modes, respectively, determined such as $d^2 n_{HS}(T)/d^2 T=0$. The dependences of the temperature T_{equ} and thermal hysteresis width δT on J_0, J_1, and J_2 are reported in Figs. 11 and 12, respectively. J_0, which is the mean LJ potential depth, does not seem to play a key role in our model. T_{equ} and δT are barely affected by large changes in J_0 except for very small values of J_0 (not shown here). J_2 drives the abruptness of the transition and the opening of the hysteresis loop. J_1, which corresponds to the difference in HS and LS potential depth and therefore to the stiffness difference between the LS and HS phases, controls mainly the position of the equilibrium temperature. This latter is therefore independent of the constant A_{HL}. In the mean-field thermodynamic model of Slichter and Drickamer,[16] there is a Γ_c critical value of the phenomenological interaction parameter Γ beyond which a thermal hysteresis can be observed. As shown in Fig. 12, such a critical value of the interaction parameter J_2 also exists in the anharmonic Ising-like model.

IV. DISCUSSION AND CONCLUSION

We have presented an Ising-like model for spin transition systems, taking into consideration the long-range elastic interactions together with the vibronic degeneracy of the HS and LS molecules. The model allows for molecular displacements governed by intermolecular Lennard-Jones potentials on a deformable lattice. By means of Monte Carlo simulations, we have analyzed the static behavior of the model; the dynamic properties will be published in a forthcoming paper. The main advantage of our approach with respect to other Ising-like schemes is the use of two coupled degrees of freedom, namely, the spin component and the lattice spacing. Within our model, the interaction between a pair of neighboring molecules in the crystal is dependent not only on their spin states but also on their separation distance, introducing explicitly inhomogeneities and a distribution of interaction constants. One key element of the model is the spin dependence of the LJ potentials; a broader potential has been attached to the HS state, corresponding to a lower bulk modulus. The HS-LS difference in potential depth controls the thermal transition temperature and behaves as an additional entropy term, attributed phenomenologically to a lattice phonon contribution. The intermolecular coupling constant J_2 drives the first-order character of the transition and width of the hysteresis loop for strong interactions. The anharmonicity (asymmetry) of the lattice, provided by the chosen LJ form of the pairwise interaction potentials, brings important aspects. For instance, thermal contraction effects, as observed and characterized experimentally, emerge directly. From a

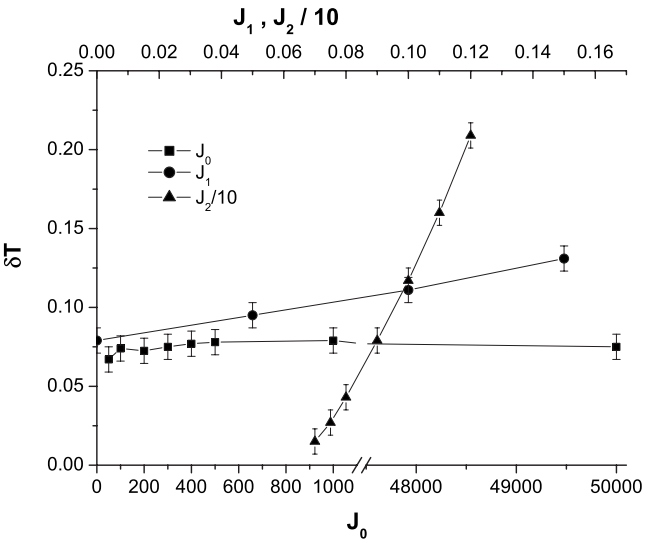

FIG. 12. Evolutions of the thermal hysteresis width δT as a function of J_0, J_1, and J_2 for $\Delta=4$.

1D analytical treatment of our anharmonic model, it will be shown in a forthcoming paper that the anharmonic contribution (by comparison with harmonic pairwise potentials) lowers the transition temperature, thus stabilizing the HS phase. It corresponds formally to additional degeneracies of lattice vibration origin in the effective field. Similar conclusions have been drawn in the case of the 1D atom-phonon coupling model. It has been shown that the anharmonic correction to the harmonic intersite coupling lowers also the transition temperature and drives the abruptness of the transition.[33]

We may anticipate that our model would allow an interpretation of the first-order transition mechanism through like-spin domain nucleation and growth, as clearly evidenced by several x-ray- and neutron-diffraction measurements. As a matter of fact, for strong intermolecular interactions, the distribution of lattice spacing presents a double sharp structure, centered on the HS and LS equilibrium distances. This is direct evidence for phase separation in the crystallographic sense. On the contrary, in the spin-crossover case (weak intermolecular coupling), the distribution of lattice spacing scales with the fraction of HS molecules. In this formalism, the notion of like-spin domains emerges from the lattice variable. This behavior contrasts with other elastic models with only long-range interactions and mean-field behavior,[37] which do not exhibit cluster growth and phase separation. It is well known that the usual Ising model with short-range interactions also exhibits cluster growth, but in this case, only spin variables are concerned: it does not correspond to a crystallographic phase separation such as the one evidenced in the present study.

Our model may be easily adapted to treat dilution (or doping) effects, that is, the case for which the crystal lattice contains both SC and non-SC molecules with different lattice spacings. Especially the influence of the strain induced by the doping elements on the dynamic behavior would be highly relevant. This possibility will be explored in a future work.

ACKNOWLEDGMENTS

This work was supported by the European Network of Excellence MAGMANet (Grant No. FP6-515767-2), the Université Henri Poincaré, and the CNRS. The authors would like to thank K. Boukheddaden for helpful discussion. Part of the numerical calculations was performed at the computing center of the Institut Jean Barriol, Nancy, which is acknowledged.

*Corresponding author; sebastien.pillet@lcm3b.uhp-nancy.fr

[1] P. Gütlich, A. Hauser, and H. Spiering, Angew. Chem., Int. Ed. Engl. **33**, 2024 (1994).
[2] *Topics in Current Chemistry*, edited by P. Gütlich and H. A. Goodwin (Springer-Verlag, Berlin, 2004), Vols. 233–235.
[3] P. Guionneau, M. Marchivie, G. Bravic, J.-F. Létard, and D. Chasseau, *Topics in Current Chemistry* (Springer-Verlag, Berlin, 2004), Vol. 233, p. 97.
[4] S. Decurtins, P. Gütlich, C. P. Köhler, and H. Spiering, Chem. Phys. Lett. **105**, 1 (1984).
[5] A. Hauser, Chem. Phys. Lett. **124**, 543 (1986).
[6] A. Hauser, Comments Inorg. Chem. **17**, 17 (1995).
[7] E. Freysz, S. Montant, S. Létard, and J.-F. Létard, Chem. Phys. Lett. **394**, 318 (2004).
[8] S. Bonhommeau, G. Molnar, A. Galet, A. Zwick, J. A. Real, J. J. McGarvey, and A. Bousseksou, Angew. Chem., Int. Ed. **44**, 4069 (2005).
[9] N. Willenbacher and H. Spiering, J. Phys. C **21**, 1423 (1988).
[10] H. Spiering and N. Willenbacher, J. Phys.: Condens. Matter **1**, 10089 (1989).
[11] H. Spiering, *Topics in Current Chemistry* (Springer-Verlag, Berlin, 2004), Vol. 235, p. 171.
[12] A. Hauser, Chem. Phys. Lett. **192**, 65 (1992).
[13] A. Hauser, J. Jeftic, H. Romstedt, R. Hinek, and H. Spiering, Coord. Chem. Rev. **190-192**, 471 (1999).
[14] J. Kroeber, J. P. Audiere, R. Claude, E. Codjovi, O. Kahn, J. G. Haasnoot, F. Groliere, C. Jay, A. Bousseksou, J. Linares, F. Varret, and A. G. Vassal, Chem. Mater. **6**, 1404 (1994).
[15] J. A. Real, A. B. Gaspar, V. Niel, and M. C. Munoz, Coord. Chem. Rev. **236**, 121 (2003).
[16] C. T. Slichter and H. G. Drickamer, J. Chem. Phys. **56**, 2142 (1972).
[17] H. Spiering, K. Boukheddaden, J. Linares, and F. Varret, Phys. Rev. B **70**, 184106 (2004).
[18] J. Wajnflasz, Phys. Status Solidi **40**, 537 (1970).
[19] J. Wajnflasz and R. Pick, J. Phys. Colloq. **32**, C1-91 (1971).
[20] A. Bousseksou, H. Constant-Machado, and F. Varret, J. Phys. I **5**, 747 (1995).
[21] K. Boukheddaden, I. Shteto, B. Hôo, and F. Varret, Phys. Rev. B **62**, 14796 (2000).
[22] K. Boukheddaden, I. Shteto, B. Hôo, and F. Varret, Phys. Rev. B **62**, 14806 (2000).
[23] F. Varret, S. A. Salunke, K. Boukheddaden, A. Bousseksou, E. Codjovi, C. Enachescu, and J. Linares, C. R. Chim. **6**, 385 (2003).
[24] M. Nishino, S. Miyashita, and K. Boukheddaden, J. Chem. Phys. **118**, 4594 (2003).
[25] K. Boukheddaden, J. Linares, E. Codjovi, F. Varret, V. Niel, and J. A. Real, J. Appl. Phys. **93**, 7103 (2003).
[26] K. Boukheddaden, J. Linares, R. Tanasa, and C. Chong, J. Phys.: Condens. Matter **19**, 106201 (2007).
[27] M. Nishino, K. Boukheddaden, S. Miyashita, and F. Varret, Phys. Rev. B **68**, 224402 (2003).
[28] H. Bolvin and O. Kahn, Chem. Phys. **192**, 295 (1995).
[29] K. Boukheddaden, J. Linares, H. Spiering, and F. Varret, Eur. Phys. J. B **15**, 317 (2000).
[30] J. A. Nasser, Eur. Phys. J. B **21**, 3 (2001).
[31] J. A. Nasser, K. Boukheddaden, and J. Linares, Eur. Phys. J. B **39**, 219 (2004).
[32] K. Boukheddaden, S. Miyashita, and M. Nishino, Phys. Rev. B **75**, 094112 (2007).
[33] K. Boukheddaden, Prog. Theor. Phys. **112**, 205 (2004).

[34] M. Nishino, K. Boukheddaden, Y. Konishi, and S. Miyashita, Phys. Rev. Lett. **98**, 247203 (2007).
[35] K. Boukheddaden, M. Nishino, and S. Miyashita., Phys. Rev. Lett. **100**, 177206 (2008).
[36] Y. Konishi, H. Tokoro, M. Nishino, and S. Miyashita, Phys. Rev. Lett. **100**, 067206 (2008).
[37] S. Miyashita, Y. Konishi, M. Nishino, H. Tokoro, and P. A. Rikvold, Phys. Rev. B **77**, 014105 (2008).
[38] S. Pillet, V. Legrand, M. Souhassou, and C. Lecomte, Phys. Rev. B **74**, 140101(R) (2006).
[39] N. Huby, L. Guérin, E. Collet, L. Toupet, J. C. Ameline, H. Cailleau, T. Roisnel, T. Tayagaki, and K. Tanaka, Phys. Rev. B **69**, 020101(R) (2004).
[40] S. Pillet, J. Hubsch, and C. Lecomte, Eur. Phys. J. B **38**, 541 (2004).
[41] K. Ichiyanagi, J. Hebert, L. Toupet, H. Cailleau, P. Guionneau, J.-F. Létard, and E. Collet, Phys. Rev. B **73**, 060408(R) (2006).
[42] Z. Xi, B. Chakraborty, K. W. Jacobsen, and J. K. Norskov, J. Phys.: Condens. Matter **4**, 7191 (1992).
[43] M. Nielsen, L. Miao, J. H. Ipsen, O. G. Mouritsen, and M. J. Zuckermann, Phys. Rev. E **54**, 6889 (1996).
[44] D. J. Bergman and B. I. Herpin, Phys. Rev. B **13**, 2145 (1976).
[45] S. Doniach, J. Chem. Phys. **68**, 4912 (1978).
[46] E. H. Boubcheur and H. T. Diep, J. Appl. Phys. **85**, 6085 (1999).
[47] P. Massimino and H. T. Diep, J. Appl. Phys. **87**, 7043 (2000).
[48] E. H. Boubcheur, P. Massimino, and H. T. Diep, J. Magn. Magn. Mater. **223**, 163 (2001).
[49] G. Molnar, V. Niel, A. B. Gaspar, J. A. Real, A. Zwick, A. Bousseksou, and J. J. McGarvey, J. Phys. Chem. B **106**, 9701 (2002).
[50] R. Zimmermann and E. Konig, J. Phys. Chem. Solids **38**, 779 (1977).
[51] V. Legrand, S. Pillet, C. Carbonera, M. Souhassou, J.-F. Létard, P. Guionneau, and C. Lecomte, Eur. J. Inorg. Chem. **2007**, 5693.
[52] A. J. Stone, *The Theory of Intermolecular Forces* (Clarendon, Oxford, 1996).
[53] T. F. Middleton, J. Hernández-Rojas, P. N. Mortenson, and D. J. Wales, Phys. Rev. B **64**, 184201 (2001).
[54] K. Nakano, S. Kawata, K. Yoneda, A. Fuyuhiro, T. Yagi, S. Nasu, S. Moritomo, and S. Kaizaki, Chem. Commun. **2004**, 2892.
[55] J. Linares, H. Spiering, and F. Varret, Eur. Phys. J. B **10**, 271 (1999).
[56] R. Boca, M. Boca, L. Dlhan, K. Falk, H. Fuess, W. Haase, R. Jarosciak, B. Papankova, F. Renz, M. Vrbova, and R. Werner, Inorg. Chem. **40**, 3025 (2001).
[57] N. Metropolis, A. W. Rosenbluth, M. N. Rosenbluth, A. H. Teller, and E. Teller, J. Chem. Phys. **21**, 1087 (1953).
[58] L. Onsager, Phys. Rev. **65**, 117 (1944).
[59] Finite-size and boundary effects remove the singularity parts of the free-energy density f_{Ising}. This in turns move away the critical temperature from the critical point which exists rigorously in the thermodynamic limit, when $N \rightarrow \infty$.
[60] A. Goujon, B. Gillon, A. Debede, A. Cousson, A. Gukasov, J. Jeftic, G. J. McIntyre, and F. Varret, Phys. Rev. B **73**, 104413 (2006).